

## Extrapolating the thermodynamic length with finite-time measurements

Jin-Fu Chen<sup>1,2</sup>, C. P. Sun<sup>1,2,\*</sup> and Hui Dong<sup>2,†</sup>

<sup>1</sup>Beijing Computational Science Research Center, Beijing 100193, China

<sup>2</sup>Graduate School of China Academy of Engineering Physics, No. 10 Xibeiwang East Road, Haidian District, Beijing 100193, China

 (Received 21 January 2021; revised 25 August 2021; accepted 27 August 2021; published 13 September 2021)

The thermodynamic length, though providing a lower bound for the excess work required in a finite-time thermodynamic process, is determined by the properties of the equilibrium states reached by the quasistatic process and is thus beyond the direct experimental measurement. We propose an experimental strategy to measure the thermodynamic length of an open classical or quantum system by extrapolating finite-time measurements. The current proposal enables the measurement of the thermodynamic length for a single control parameter without requiring extra effort to find the optimal control scheme, and is illustrated with examples of the quantum harmonic oscillator with tuning frequency and the classical ideal gas with changing volume. Such a strategy shall shed light on the experimental design of the lacking platforms to measure the thermodynamic length.

DOI: [10.1103/PhysRevE.104.034117](https://doi.org/10.1103/PhysRevE.104.034117)

### I. INTRODUCTION

Optimization of thermodynamic processes is of great importance in finite-time thermodynamics [1–3] to minimize the dissipation [4,5] and to improve the performance of heat engines [6–16]. The extent to which the optimization is achieved is discovered to be limited by the geometric properties of the space of thermodynamic equilibrium states [17–22] and provides a criterion for the amelioration of specific control schemes. For a finite-time process with the operation time  $\tau$ , the optimization is realized by minimizing the entropy production [7,23–25] or the excess work  $W_{\text{ex}}$  [5,26,27], which is bounded as  $W_{\text{ex}} \geq \mathcal{L}^2/\tau$  [20,21,28–31] at the long-time limit. The thermodynamic length  $\mathcal{L}$ , appearing constantly in both classical and quantum systems [3,21,31–39], is related to the geometric metric of the equilibrium states [21,30,31,40–42].

However, it remains a challenge to practically measure the length in thermodynamic processes. To obtain the geometry metric, one needs the exact equilibrium thermal states along the path of the control parameters [20,43] through infinitely slow isothermal processes, but the measurement errors are greatly amplified with the longer operation time. In this paper, we propose to measure the thermodynamic length by extrapolating a few data points of a finite-time version  $\mathcal{L}(\tau)$ , which has the property to retain the thermodynamic length  $\mathcal{L}$  at the long-time limit. The measurement procedure is illustrated with examples of both the quantum harmonic oscillator with tuning frequency and the classical ideal gas with changing volume.

The rest of the paper is organized as follows. In Sec. II we define a finite-time version of the thermodynamic length for generic tuned open quantum systems (also applicable in classical systems). The finite-time thermodynamic length

converges to the thermodynamic length at the long-time limit, and the convergence is independent of the protocol for a single control parameter. In Sec. III we propose an extrapolation method to measure the thermodynamic length for the system with a single control parameter, and illustrate this method with examples of the quantum harmonic oscillator with tuning frequency and the classical ideal gas with changing volume. The conclusion is given in Sec. IV. Relevant derivations and discussions are given in the Appendices.

### II. FINITE-TIME THERMODYNAMIC LENGTH

We consider an open quantum system with the control parameter  $\lambda(t)$  tuned from the initial value  $\lambda(0) = \lambda_0$  to the final value  $\lambda(\tau) = \lambda_\tau$  in a finite-time process with duration  $\tau$ . The system state is described by the density matrix  $\rho(t)$  ( $0 < t < \tau$ ), which evolves under the time-dependent Hamiltonian  $H(t) = H[\lambda(t)]$  via the time-dependent Markovian master equation [44]

$$\dot{\rho} = \mathcal{L}_{\lambda(t)}\rho, \quad (1)$$

where  $\mathcal{L}_{\lambda(t)}$  is the quantum Liouvillian super-operator. In quantum thermodynamics, the rate of the performed work, namely, the power, is  $\dot{W} = \text{Tr}(\rho\dot{H})$  [45,46]. In a quasistatic isothermal process with infinite operation time, the system evolves along the trajectory of the equilibrium state  $\rho_{\text{eq}}(t) = \exp[-\beta_b H(t)]/\text{Tr}\{\exp[-\beta_b H(t)]\}$  with the inverse temperature  $\beta_b = 1/(k_B T_b)$  of the bath, and the performed work of the whole process is  $W_{(0)} = \int_{\lambda_0}^{\lambda_\tau} \text{Tr}(\rho_{\text{eq}} \partial H / \partial \lambda) d\lambda$ . In a finite-time isothermal process, the excess work  $W_{\text{ex}}(\tau) = \int_0^\tau P_{\text{ex}}(t) dt$  is utilized to evaluate the dissipation with the excess power  $P_{\text{ex}}(t) = \dot{W}(t) - \dot{W}_{(0)}(t)$ , where  $\dot{W}_{(0)}(t) = \text{Tr}[\rho_{\text{eq}} \dot{H}]$  is the quasistatic part of the work rate. One important progress [20,28,30] in finite-time thermodynamics is the discovery of the geometric bound of the excess work with the thermodynamic length as  $W_{\text{ex}}(\tau) \geq \mathcal{L}^2/\tau$ , and the equality is saturated by the optimal protocol with the constant excess

\*cpsun@gscaep.ac.cn

†hdong@gscaep.ac.cn

power. The direct measurement of thermodynamic length  $\mathcal{L}$  requires the infinitely slow isothermal processes [20,43].

In quantum thermodynamics, the thermodynamic length  $\mathcal{L}$  is explicitly [21]

$$\mathcal{L} = \int_{\lambda_0}^{\lambda_\tau} \sqrt{\text{Tr} \left[ \frac{\partial H}{\partial \lambda} \mathcal{L}_\lambda^{-1} \left( \frac{\partial \rho_{\text{eq}}}{\partial \lambda} \right) \right]} d\lambda, \quad (2)$$

which contains the Drazin inverse  $\mathcal{L}_\lambda^{-1}$  of the super-operator [47,48]. For the diagonalizable super-operator, the Drazin inverse is explicitly obtained as follows. The eigendecomposition is  $\mathcal{L}_\lambda = \sum_\Gamma \Gamma P_\Gamma$  with the eigenvalues  $\Gamma$  and the projections  $P_\Gamma$  in the super-space of the density matrices. The null eigenvector is the instantaneous equilibrium state satisfied  $\mathcal{L}_\lambda[\rho_{\text{eq}}(\lambda)] = 0$ . The Drazin inverse is then written as  $\mathcal{L}_\lambda^{-1} = \sum_{\Gamma \neq 0} \Gamma^{-1} P_\Gamma$ , where the inverses of the nonzero eigenvalues  $\Gamma^{-1}$  determines different dissipation timescales [47,48]. Detailed discussions about the Drazin inverse are given with an example of the two-level system in Appendix B.

For the measurement, we define a finite-time thermodynamic length as

$$\mathcal{L}(\tau) = \int_0^\tau \sqrt{P_{\text{ex}}(t)} dt. \quad (3)$$

The two following properties of the finite-time thermodynamic length allows measuring the thermodynamic length by extrapolating finite-time measurements.

(i) *The convergence*  $\lim_{\tau \rightarrow \infty} \mathcal{L}(\tau) = \mathcal{L}$ : In a slow isothermal process, the state of the system evolves near the equilibrium state, and the solution to Eq. (1) is expanded in the series [49] as

$$\rho(t) = \sum_{n=0}^{\infty} \left( \mathcal{L}_{\lambda(t)}^{-1} \frac{d}{dt} \right)^n \rho_{\text{eq}}(t). \quad (4)$$

For a given protocol  $\lambda(t) = \tilde{\lambda}(t/\tau)$ , the series expansion of the excess power is obtained as

$$P_{\text{ex}}(t) = \text{Tr} \left\{ \frac{\partial \tilde{H}(s)}{\partial s} \sum_{n=1}^{\infty} \frac{1}{\tau^{n+1}} \left( \mathcal{L}_{\tilde{\lambda}(s)}^{-1} \frac{\partial}{\partial s} \right)^n [\tilde{\rho}_{\text{eq}}(s)] \right\}, \quad (5)$$

where  $s = t/\tau$  is the rescaled dimensionless time. Equation (5) is invalid at the beginning of the isothermal process. Its validity requires the evolution time larger than the typical dissipation timescale. For the slow process, the lowest-order term with  $n = 1$  dominates the summation, and the finite-time thermodynamic length approaches the thermodynamic length at the long-time limit.

(ii) *The protocol independence of the limit*  $\lim_{\tau \rightarrow \infty} \mathcal{L}(\tau)$ : For the system with only one control parameter, the limit of the finite-time thermodynamic length  $\lim_{\tau \rightarrow \infty} \mathcal{L}(\tau)$  is independent of the protocol, which implies the thermodynamic length can be measured without necessarily using the optimal protocol. For multiple control parameters, the limit  $\lim_{\tau \rightarrow \infty} \mathcal{L}(\tau)$  indeed relies on the path of the protocol. The minimal thermodynamic length is only reached by the geodesic path, and the optimized protocol is to tune the control parameter with the constant velocity of the thermodynamic length [21].

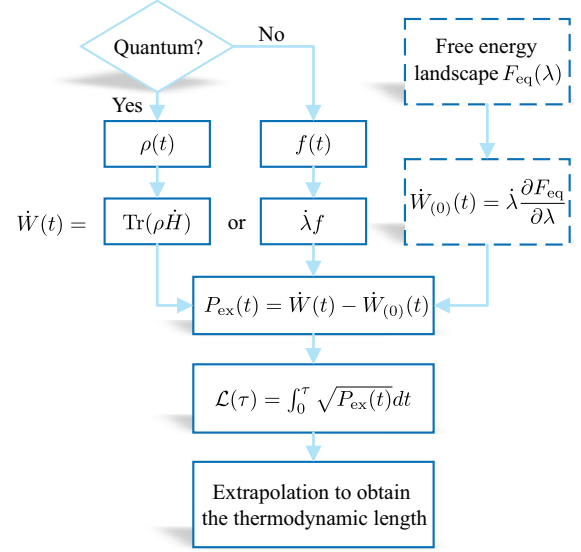


FIG. 1. Flowchart for measuring the thermodynamic length  $\mathcal{L}$  with finite-time extrapolation. The excess power is evaluated with the performed work rate  $\dot{W}(t)$  and the quasistatic work rate  $\dot{W}_{(0)}(t)$  at each moment of the finite-time process.

### III. MEASURING THE THERMODYNAMIC LENGTH THROUGH EXTRAPOLATION

The thermodynamic length is the long-time limit of the finite-time thermodynamic length. In the following, we propose an extrapolation method to measure the thermodynamic length for the system with a single control parameter. The flowchart of the method is shown in Fig. 1. The measurement of the finite-time thermodynamic length  $\mathcal{L}(\tau)$  requires the excess power  $P_{\text{ex}}(t)$  of the whole process. The power  $\dot{W}(t)$  ( $0 < t < \tau$ ) in a finite-time process is measured through the conjugate force  $f(t) = \text{Tr}[\rho \partial_\lambda H]$  for a classical system via  $\dot{W}(t) = \dot{\lambda}(t)f(t)$  or the tomography of the density matrix  $\rho(t)$  for a quantum system via  $\dot{W}(t) = \text{Tr}(\rho \dot{H})$ . With the given protocol  $\tilde{\lambda}(s)$  of the control parameter, the quasistatic work rate  $\dot{W}_{(0)}(t) = \text{Tr}(\rho_{\text{eq}} \dot{H}) = \dot{\lambda} \partial_\lambda F_{\text{eq}}(\lambda)$  is obtained with the landscape of the equilibrium free energy  $F_{\text{eq}}(\lambda)$ , which can be typically obtained from finite-time processes via Jarzynski's equality [50].

Assuming the length  $\mathcal{L}(\tau)$  as a smooth function of the operation time  $\tau$ , we expand  $\mathcal{L}(\tau)$  into the Laurent series

$$\mathcal{L}(\tau) = \mathcal{L} + \sum_{j=1}^{\infty} \frac{a_j}{\tau^j}. \quad (6)$$

The operation time  $\tau$  needs to be chosen notably larger than the dissipation timescale to ensure the validity of Eq. (5). By measuring the finite-time thermodynamic length under the given operation time, we extrapolate the function as  $\mathcal{L}(\tau) = \mathcal{L} + \sum_{j=1}^N a_j \tau^{-j}$  with the cutoff  $N$ . The thermodynamic length  $\mathcal{L}$  is estimated with the extrapolation  $\tau \rightarrow \infty$ . We apply the current strategy to measure the thermodynamic length with two examples, the quantum harmonic oscillator and the classical ideal gas system.

### A. Quantum harmonic oscillator with tuned frequency

We consider the quantum Brownian motion with the Hamiltonian  $H(t) = \hat{p}^2/(2m) + m\omega(t)^2\hat{x}^2/2$  in a tuned harmonic potential with the frequency  $\omega(t)$  as the control parameter in the finite-time isothermal process. At the high-temperature limit, the evolution of the reduced system is described by the Caldeira-Leggett master equation [44,51], i.e.,  $\partial_t \rho = \mathcal{L}_{\omega(t)} \rho$ . The quantum Liouvillian super-operator is explicitly

$$\mathcal{L}_{\omega(t)} \rho = -i[H(t), \rho] - i\kappa[\hat{x}, \{\hat{p}, \rho\}] - \frac{2m\kappa}{\beta_b}[\hat{x}, [\hat{x}, \rho]], \quad (7)$$

where the frequency-independent damping rate  $\kappa$  is induced by the Ohmic spectral of the heat bath [44,51].

With the infinite dimension of the Hilbert space for a harmonic oscillator, it is difficult to solve the evolution of the density matrix by calculating the Drazin inverse of the super-operator directly. An alternative way is to solve the finite-time dynamics via a closed Lie algebra [52,53] with the thermodynamic variables, the Hamiltonian  $H(t)$ , the Lagrange  $L(t) = \hat{p}^2/(2m) - m\omega(t)^2\hat{x}^2/2$ , and the correlation function  $D(t) = \omega(t)(\hat{x}\hat{p} + \hat{p}\hat{x})/2$ . The closed differential equations of the expectations of the thermodynamic variables  $\langle H(t) \rangle = \text{Tr}[\rho(t)H(t)]$ ,  $\langle L(t) \rangle = \text{Tr}[\rho(t)L(t)]$ , and  $\langle D(t) \rangle = \text{Tr}[\rho(t)D(t)]$  are obtained from Eq. (7) as

$$\begin{aligned} \frac{d}{dt} \begin{pmatrix} \langle H \rangle \\ \langle L \rangle \\ \langle D \rangle \end{pmatrix} &= \begin{pmatrix} -2\kappa + \frac{\dot{\omega}}{\omega} & -2\kappa - \frac{\dot{\omega}}{\omega} & 0 \\ -2\kappa - \frac{\dot{\omega}}{\omega} & -2\kappa + \frac{\dot{\omega}}{\omega} & -2\omega \\ 0 & 2\omega & -2\kappa + \frac{\dot{\omega}}{\omega} \end{pmatrix} \begin{pmatrix} \langle H \rangle \\ \langle L \rangle \\ \langle D \rangle \end{pmatrix} \\ &+ 2\kappa k_B T_b \begin{pmatrix} 1 \\ 1 \\ 0 \end{pmatrix}. \end{aligned} \quad (8)$$

The derivation to Eq. (8) is presented in Appendix C.

The performed work rate of the tuned harmonic oscillator is  $\dot{W} = \dot{\omega}/\omega(\langle H \rangle - \langle L \rangle)$ . In a quasistatic isothermal process, the system evolves along the equilibrium states with the average internal energy  $\langle H \rangle = k_B T_b$  and the average Lagrange  $\langle L \rangle = 0$ , and the quasistatic work rate is  $\dot{W}_{(0)}(t) = k_B T_b \dot{\omega}/\omega$ . In a finite-time process, the finite-time thermodynamic length  $\mathcal{L}(\tau)$  is explicitly

$$\mathcal{L}(\tau) = \int_0^\tau \left[ \frac{\dot{\omega}}{\omega} (\langle H \rangle - \langle L \rangle - k_B T_b) \right]^{1/2} dt. \quad (9)$$

The thermodynamic length of the tuned harmonic oscillator is obtained by Eq. (2) as

$$\mathcal{L} = \sqrt{\frac{k_B T_b}{2\kappa}} \left[ \sinh^{-1} \left( \frac{\omega}{2\kappa} \right) - \sqrt{1 + \frac{4\kappa^2}{\omega^2}} \right] \Big|_{\omega=\omega_0}^{\omega_\tau}, \quad (10)$$

where  $\omega_0$  and  $\omega_\tau$  are the initial and final frequencies of the harmonic potential. The detailed derivation of the thermodynamic length is given in Appendix C. The optimal protocol  $\omega_{\text{op}}(t) = \tilde{\omega}_{\text{op}}(t/\tau)$  satisfies

$$\left( \frac{1}{2\kappa} + \frac{2\kappa}{\tilde{\omega}_{\text{op}}^2} \right)^{1/2} \frac{1}{\tilde{\omega}_{\text{op}}} \frac{d\tilde{\omega}_{\text{op}}}{ds} = \text{const.} \quad (11)$$

In the underdamped limit  $\kappa/\omega \ll 1$ , the thermodynamic length approximates  $\mathcal{L} \approx \sqrt{k_B T_b/(2\kappa)} |\ln \omega_\tau/\omega_0|$ , and the

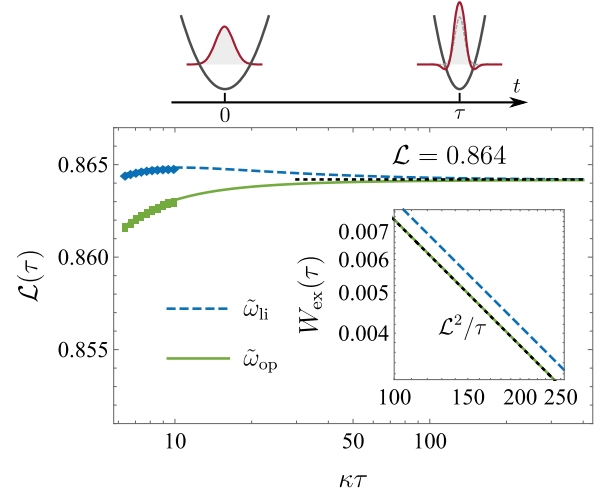


FIG. 2. Finite-time extrapolation to measure the thermodynamic length for the quantum Brownian motion in a tuned harmonic potential. With the current chosen parameters, the black dotted line presents the thermodynamic length  $\mathcal{L} = 0.864$ . It is approached by the extrapolated functions with  $N = 3$  for both the linear (blue dashed curve) and the optimal (green solid curve) protocols. The inset shows the excess work in a slow process is bounded as  $W_{\text{ex}}(\tau) \geq \mathcal{L}^2/\tau$  (black dotted line), which is saturated by the optimal protocol at the long-time limit.

optimal protocol is the exponential protocol  $\tilde{\omega}_{\text{op}}(s) = \omega_0 \exp[s \ln(\omega_\tau/\omega_0)]$ . In the overdamped limit  $\kappa/\omega \gg 1$ , the thermodynamic length approximates  $\mathcal{L} \approx \sqrt{2\kappa k_B T_b} |(\omega_\tau - \omega_0)/(\omega_0 \omega_\tau)|$ , and the optimal protocol is the inverse protocol  $\tilde{\omega}_{\text{op}}(s) = \omega_0 \omega_\tau / [(\omega_0 - \omega_\tau)s + \omega_\tau]$ .

We exemplify the finite-time extrapolation method to obtain the thermodynamic length of the tuned harmonic oscillator through numerically solving the relaxation dynamics with the linear protocol  $\tilde{\omega}_{\text{li}}(s) = \omega_0 + (\omega_\tau - \omega_0)s$  and the optimal protocol  $\tilde{\omega}_{\text{op}}(s)$ . In the numerical calculation, the frequency is tuned from  $\omega_0 = 1$  to  $\omega_\tau = 2$  with the temperature  $k_B T_b = 1$  and the damping rate  $\kappa = 1$ . In Fig. 2 the extrapolated functions (curves) with  $N = 3$  are obtained from 10 sets of data (markers) with the operation time  $\tau$  ranging from 6.4 to 9.9 for the linear (blue dashed line) and the optimal (green solid line) protocols as  $\mathcal{L}_{\text{li}}(\tau) = 0.864 + 0.0128/\tau - 0.0464/\tau^2 - 0.145/\tau^3$  and  $\mathcal{L}_{\text{op}}(\tau) = 0.864 - 0.00471/\tau - 0.0448/\tau^2 - 0.168/\tau^3$ . The two extrapolated functions both give the consistent thermodynamic length identical to the theoretical result  $\mathcal{L} = 0.864$  by Eq. (10), as illustrated with the dotted black line. Therefore, the current extrapolation method enables the measurement of the thermodynamic length in relatively short time without finding the optimal protocol. The inset shows the  $\tau^{-1}$  scaling of the excess work. The excess work of both the linear (blue dashed) and the optimal (green solid) protocols is indeed bounded by the thermodynamic length (black dotted line), and the bound is saturated by the optimal protocol.

### B. Compression of classical ideal gas

The extrapolation method is applicable in classical systems with the strategy shown in Fig. 1. We consider the finite-time

compression of the classical ideal gas in a cylinder, which is in contact with a heat bath at the temperature  $T_b$ . By compressing the piston, the volume of the cylinder changes with the performed work rate  $\dot{W} = -p\dot{V}$ , where  $p$  and  $V$  are the pressure of the gas and the volume of the cylinder. As derived in Ref. [54], the temperature  $T$  of the classical ideal gas satisfies

$$\frac{dT}{dt} = -\frac{nRT}{C_V} \frac{1}{V} \frac{dV}{dt} - \gamma(T - T_b), \quad (12)$$

where  $n$  is the number of moles of gas and  $R$  is the ideal gas constant,  $\gamma$  is the cooling rate in Newton's law of cooling, assumed as a constant in the following discussion, and  $C_V$  is the heat capacity at the constant volume, e.g.,  $C_V = 3nR/2$  for the single-atom ideal gas. In a finite-time isothermal process, the excess power is obtained as  $P_{\text{ex}}(t) = -nR(T - T_b)\dot{V}/V$ . The finite-time thermodynamic length is measured as

$$\mathcal{L}(\tau) = \int_0^\tau \sqrt{-\left[p(t) - \frac{p(0)V(0)}{V(t)}\right]\dot{V}(t)} dt. \quad (13)$$

At the long-time limit, the thermodynamic length  $\mathcal{L}$  is theoretically obtained as

$$\mathcal{L} = \sqrt{\frac{(nR)^2 T_b}{\gamma C_V}} \left| \ln \frac{V_\tau}{V_0} \right|, \quad (14)$$

where  $V_0$  and  $V_\tau$  are the initial and final volume of the cylinder. For a long-time compression process, the optimal protocol with the constant excess power is obtained as the exponential protocol  $\tilde{V}_{\text{op}}(s) = V_0(V_\tau/V_0)^s$ , which is consistent with the result obtained by the stochastic thermodynamics [55].

In Fig. 3 the finite-time thermodynamic lengths (markers) for given protocols are numerically obtained for the isothermal processes with the operation time  $\tau$  ranging from 11.0 to 20.0, where the parameters are set as  $nR = T_b = \gamma = 1$  and  $C_V = 1.5$ . We adopt the linear protocol  $\tilde{V}_{\text{li}}(s) = 1 - s/2$  (blue dashed curve) and the optimal protocol  $\tilde{V}_{\text{op}}(s) = 2^{-s}$  (green solid curve) to compressing the volume of the cylinder from  $V_0 = 1$  to  $V_\tau = 0.5$ . Setting the cutoff  $N = 3$ , the extrapolated functions of the two protocols are obtained as  $\mathcal{L}_{\text{li}}(\tau) = 0.566 - 0.318/\tau + 0.010/\tau^2 - 0.146/\tau^3$  and  $\mathcal{L}_{\text{op}}(\tau) = 0.566 - 0.216/\tau - 0.199/\tau^2 - 0.111/\tau^3$ . The extrapolations with different protocols lead to the same value, matching the theoretical result  $\mathcal{L} = 0.566$  (black dotted line) given by Eq. (14).

To clarify the importance of the extrapolation, we consider the experimental measurement errors, e.g., the calibration errors and electronic noise. These errors dominate the results during the direct measurement of the thermodynamic length due to the fundamental properties of the integration over the vanishing measurement kernel, namely  $P_{\text{ex}}(t) \sim 0$  for any  $t \in [0, \tau]$  in a long-time process. Here we consider the measured pressure contains  $10^{-5}$  calibration error. Such a small error is amplified with the increase of the operation time, as illustrated by the thin curves in Fig. 3. The extrapolation is the only method overcome the above problem by measure the finite-time thermodynamic length with the short-time experimental data affected by these errors. The detailed discussion is left for Appendix D.

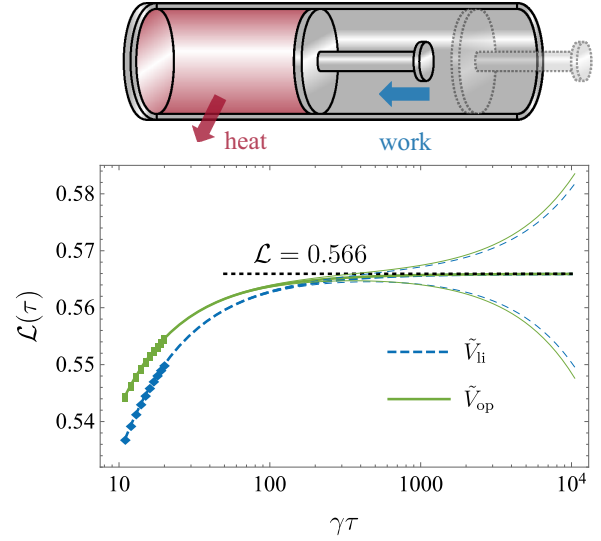


FIG. 3. Finite-time extrapolation to measure the thermodynamic length for the compression of the classical ideal gas in a cylinder. We adopt the linear protocol (blue dashed curve) and the optimal protocol (green solid curve) to compress the volume of the cylinder to one half. With the current chosen parameters, the length extrapolated with the two protocols match the exact thermodynamic length  $\mathcal{L} = 0.566$  (black dotted line) by Eq. (14). The thin curves show the effect of the calibration error on the finite-time thermodynamic length, where we consider  $10^{-5}$  calibration error to exist in the measured pressure.

Using examples of both the quantum harmonic oscillator and the classical ideal gas, we demonstrate the proposed extrapolation method for measuring the thermodynamic length for typical systems with a single control parameter. The quantum harmonic oscillator has been potentially realized with the trapped ion [56,57], and the classical ideal gas system will be tested with our recently designed apparatus [54].

#### IV. CONCLUSION

The thermodynamic length is crucial in the optimization of finite-time thermodynamic processes, yet remains challenging to be practically measured in experiments. We propose to measure the thermodynamic length via the finite-time extrapolation method. The protocol-independent property of the current measurement strategy benefits to practically measure the thermodynamic length directly with simple and realizable control schemes in possible experimental platforms. The current measurement proposal shall pave the way for measuring the thermodynamic length with various experimental platforms, which is still lacking for the finite-time thermodynamic studies.

#### ACKNOWLEDGMENTS

J.-F.C. thanks Ruo-Xun Zhai for the helpful discussions about the dry-air experiment. This work is supported by the National Natural Science Foundation of China (NSFC) (Grants No. 11534002, No. 11875049, No. U1930402, No. U1930403, and No. 12088101) and the National Basic Research Program of China (Grant No. 2016YFA0301201).

### APPENDIX A: CONVERGENCE OF THE FINITE-TIME THERMODYNAMIC LENGTH

We demonstrate the convergence of the finite-time thermodynamic length  $\mathcal{L} = \lim_{\tau \rightarrow \infty} \mathcal{L}(\tau)$ . Plugging the series expansion of the excess power by Eq. (5) into Eq. (3), the finite-time thermodynamic length is rewritten as

$$\mathcal{L}(\tau) = \int_0^1 \sqrt{\sum_{n=1}^{\infty} \text{Tr} \left[ \frac{\partial \tilde{H}(s)}{\partial s} \tau^{1-n} \left( \mathcal{L}_{\tilde{\lambda}(s)}^{-1} \frac{\partial}{\partial s} \right)^n \tilde{\rho}_{\text{eq}}(s) \right]} ds. \quad (\text{A1})$$

With the increasing control time  $\tau$ , the term with  $n = 1$  is independent of  $\tau$  and dominates the summation, and leads to the thermodynamic length

$$\mathcal{L} = \int_0^1 \sqrt{\text{Tr} \left[ \frac{\partial \tilde{H}}{\partial s} \left( \mathcal{L}_{\tilde{\lambda}(s)}^{-1} \frac{\partial}{\partial s} \right) \tilde{\rho}_{\text{eq}} \right]} ds \quad (\text{A2})$$

$$= \int_0^1 \sqrt{[\tilde{\lambda}'(s)]^2 \text{Tr} \left[ \left( \frac{\partial H}{\partial \lambda} \right) \left( \mathcal{L}_{\tilde{\lambda}(s)}^{-1} \frac{\partial \tilde{\rho}_{\text{eq}}}{\partial \lambda} \right) \right]} ds \quad (\text{A3})$$

$$= \int_{\lambda_0}^{\lambda_1} \sqrt{\text{Tr} \left[ \left( \frac{\partial H}{\partial \lambda} \right) \left( \mathcal{L}_{\lambda}^{-1} \frac{\partial \rho_{\text{eq}}}{\partial \lambda} \right) \right]} |d\lambda|. \quad (\text{A4})$$

The last integral shows  $\mathcal{L}$  is independent of the protocol  $\tilde{\lambda}(s)$  for tuning a single control parameter.

### APPENDIX B: TWO-LEVEL SYSTEM WITH TUNED ENERGY SPACING

In this section, we show the example of the two-level system with the tuned energy spacing. The Drazin inverse of the super-operator is obtained directly for the optimization of the protocol. The system Hamiltonian of the two-level system reads

$$H(t) = \frac{E(t)}{2} (|e\rangle\langle e| - |g\rangle\langle g|), \quad (\text{B1})$$

where the energy spacing  $E(t)$  is the control parameter. The state of the two-level system is represented with the density matrix

$$\rho(t) = \begin{pmatrix} \rho_{ee} & \rho_{eg} \\ \rho_{ge} & \rho_{gg} \end{pmatrix}. \quad (\text{B2})$$

With the coupling to the heat bath, the evolution is governed by the time-dependent master equation

$$\dot{\rho} = \mathcal{L}_{E(t)}(\rho), \quad (\text{B3})$$

where  $\mathcal{L}_{E(t)}$  is in the Lindblad form

$$\mathcal{L}_{E(t)}(\rho) = -i[H(t), \rho] + \sum_{i=\pm} \gamma_i(t) \mathcal{D}(\sigma_i)[\rho], \quad (\text{B4})$$

with the transition operators  $\sigma_+ = |e\rangle\langle g|$ ,  $\sigma_- = |g\rangle\langle e|$  and the dissipation super-operator

$$\mathcal{D}(\sigma)[\rho] = \sigma \rho \sigma^\dagger - \frac{1}{2} \sigma^\dagger \sigma \rho - \frac{1}{2} \rho \sigma^\dagger \sigma. \quad (\text{B5})$$

The time-dependent transition rates are  $\gamma_+(t) = \gamma(t)N(t)$  and  $\gamma_-(t) = \gamma(t)[N(t) + 1]$  with the average phonon number

$$N(t) = \frac{1}{e^{\beta_b E(t)} - 1}. \quad (\text{B6})$$

The spontaneous emission rate  $\gamma(t)$  relies on the bath spectral as

$$\gamma(t) = \gamma_0 E(t)^\alpha. \quad (\text{B7})$$

Equation (B4) extends the well-known Lindblad master equation [44] for the tuned two-level system via the time-dependent energy spacing  $E(t)$ . This approximation is suitable for a long-time isothermal process with slowly tuned control parameters.

Rewriting the density matrix into a vector

$$\rho = (\rho_{ee} \quad \rho_{gg} \quad \rho_{eg} \quad \rho_{ge})^T, \quad (\text{B8})$$

the super-operator is presented in the matrix form as

$$\mathcal{L}_{E(t)} = \begin{pmatrix} -\gamma(N+1) & \gamma N & 0 & 0 \\ \gamma(N+1) & -\gamma N & 0 & 0 \\ 0 & 0 & -\gamma(N+\frac{1}{2}) - iE & 0 \\ 0 & 0 & 0 & -\gamma(N+\frac{1}{2}) + iE \end{pmatrix}, \quad (\text{B9})$$

with the eigenvalues  $\Gamma = 0, -\gamma(N+1/2) \pm iE$ , and  $\gamma(2N+1)$ . The Drazin inverse of the super-operator is obtained as

$$\mathcal{L}_{E(t)}^{-1} = \begin{pmatrix} -\frac{(N+1)}{\gamma(2N+1)^2} & \frac{N}{\gamma(2N+1)^2} & 0 & 0 \\ \frac{(N+1)}{\gamma(2N+1)^2} & -\frac{N}{\gamma(2N+1)^2} & 0 & 0 \\ 0 & 0 & \frac{1}{-\gamma(N+\frac{1}{2})-iE} & 0 \\ 0 & 0 & 0 & \frac{1}{-\gamma(N+\frac{1}{2})+iE} \end{pmatrix}. \quad (\text{B10})$$

At the time  $t$ , the instantaneous equilibrium state is

$$\rho_{\text{eq}}(t) = \left( \frac{N(t)}{2N(t)+1} \quad \frac{N(t)+1}{2N(t)+1} \quad 0 \quad 0 \right)^T. \quad (\text{B11})$$

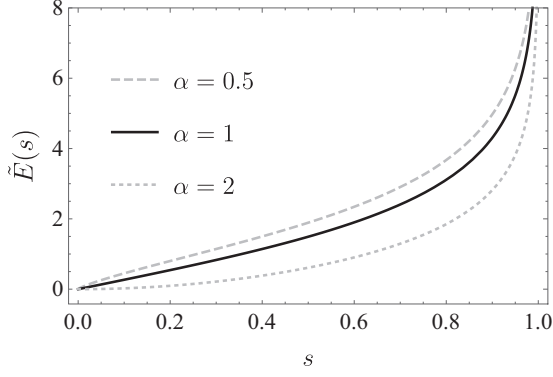


FIG. 4. The optimal protocols of tuning the energy spacing  $\tilde{E}(s)$  of the two-level system with different bath spectral  $\alpha = 0.5, 1,$  and  $2$ . The optimal protocols are obtained by numerically solving Eq. (B15) with the parameters  $\beta_b = 1$  and  $\gamma_0 = 1$ .

The off-diagonal terms of the density matrix remain zero  $\rho_{eg}(t) = \rho_{ge}^*(t) = 0$  during the whole isothermal process. The excess power to the first order is

$$P_{\text{ex}}^{[1]}(t) = \text{Tr} \left[ \frac{dH(t)}{dt} \mathcal{L}_{E(t)}^{-1} \left( \frac{d\rho_{\text{eq}}(t)}{dt} \right) \right] \quad (\text{B12})$$

$$= \frac{\beta_b \dot{E}^2 \tanh\left(\frac{1}{2}\beta_b E\right)}{4\gamma \cosh^2\left(\frac{1}{2}\beta_b E\right)}. \quad (\text{B13})$$

The thermodynamic length follows as

$$\mathcal{L} = \int_{E_0}^{E_\tau} \sqrt{\frac{\beta_b \tanh\left[\frac{1}{2}\beta_b E(t)\right]}{4\gamma_0 E^\alpha \cosh^2\left[\frac{1}{2}\beta_b E(t)\right]}} dE. \quad (\text{B14})$$

At the long-time limit, the optimal protocol  $\tilde{E}(s)$  is obtained with the constant excess power  $P_{\text{ex}}^{[1]}(t) = \text{const}$ , namely,

$$\frac{\beta_b \tanh\left[\frac{1}{2}\beta_b \tilde{E}(s)\right]}{4\gamma_0 \tilde{E}(s)^\alpha \cosh^2\left[\frac{1}{2}\beta_b \tilde{E}(s)\right]} \left[ \frac{d\tilde{E}(s)}{ds} \right]^2 = \text{const}. \quad (\text{B15})$$

Figure 4 shows the tuning of the energy spacing  $\tilde{E}(s)$  with  $s$  ranging from 0 to 1. We solve the optimal protocols for differ-

ent bath spectral, the sub-Ohmic  $\alpha = 0.5$  (dashed curve), the Ohmic  $\alpha = 1$  (dotted curve), and super-Ohmic  $\alpha = 2$  (dash-dotted curve) with the inverse temperature  $\beta_b = 1$  and the dissipation strength  $\gamma_0 = 1$ .

With the Ohmic spectral  $\alpha = 1$  of the bath, we exemplify the extrapolation method to measure the thermodynamic length of the two-level system. The energy spacing is tuned from  $E_0 = 1$  to  $E_\tau = 2$  with the linear and the optimal protocols. Figure 5(a) shows the measured finite-time thermodynamic length  $\mathcal{L}(\tau) = \int_0^\tau \sqrt{P_{\text{ex}}(t)} dt$  (markers) with the duration ranging from 10.0 to 19.0. With the cutoff  $N = 3$ , the extrapolated functions are obtained for the two protocols as  $\mathcal{L}_{\text{li}}(\tau) = 0.495 - 0.000284/\tau - 0.0179/\tau^2 - 0.0307/\tau^3$  and  $\mathcal{L}_{\text{op}}(\tau) = 0.495 - 0.0136/\tau - 0.0500/\tau^2 - 0.0130/\tau^3$ . They both approach the thermodynamic length (black dotted line) with the increasing duration  $\tau$ . Figure 5(b) shows the  $\tau^{-1}$  scaling of the excess work at the long-time limit. The excess work is bounded by the thermodynamic length as  $W_{\text{ex}} \geq \mathcal{L}^2/\tau$ . The excess work done with the optimal protocol matches the lower bound given by the thermodynamic length (black dotted line).

## APPENDIX C: QUANTUM BROWNIAN MOTION IN A TUNED HARMONIC POTENTIAL

### 1. Differential equations of the average values

We first derive the differential equation (8) of the average values of the internal energy  $\langle H(t) \rangle = \text{Tr}[\rho(t)H(t)]$ , the Lagrange  $\langle L(t) \rangle = \text{Tr}[\rho(t)L(t)]$  and the correlation function  $\langle D(t) \rangle = \text{Tr}[\rho(t)D(t)]$ . According to the Caldeira-Leggett master equation [44,51], the time derivative of the internal energy is calculated as

$$\frac{d\langle H \rangle}{dt} = m\omega(t)\dot{\omega}(t)\text{Tr}[\rho(t)\hat{x}^2] + \text{Tr}\{\mathcal{L}_{\omega(t)}[\rho(t)]H(t)\}, \quad (\text{C1})$$

where the upper dot denotes the time derivative, namely,  $\dot{\omega}(t) = d\omega/dt$ . With the similar calculation of time derivatives for the Lagrange and the correlation function,

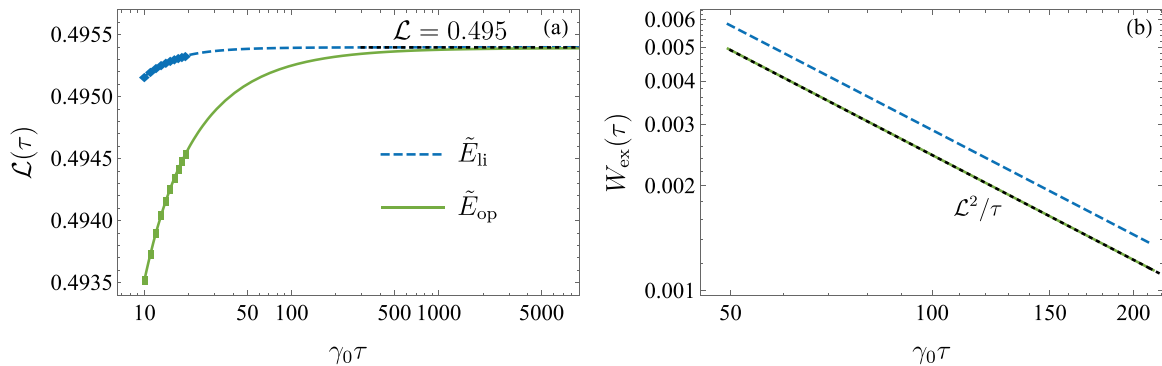


FIG. 5. Finite-time extrapolation for the two-level system with the tuned energy spacing. (a) Finite-time thermodynamic lengths for the linear and the optimal protocols. Through measuring the finite-time thermodynamic length with short duration (markers), the thermodynamic length can be approached by the extrapolated functions of both protocols. (b) The  $\tau^{-1}$  scaling of the excess work. For a long-time process, the optimal protocol (green solid line) consumes less excess work and saturates the lower bound given by the thermodynamic length (black dotted line).

we obtain the differential equations of average values as

$$\frac{d\langle H \rangle}{dt} = \frac{\dot{\omega}}{\omega}(\langle H \rangle - \langle L \rangle) - 2\kappa(\langle H \rangle + \langle L \rangle) + 2\kappa k_B T_b, \quad (\text{C2})$$

$$\frac{d\langle L \rangle}{dt} = -\frac{\dot{\omega}}{\omega}(\langle H \rangle - \langle L \rangle) - 2\omega\langle D \rangle - 2\kappa(\langle H \rangle + \langle L \rangle) + 2\kappa k_B T_b, \quad (\text{C3})$$

$$\frac{d\langle D \rangle}{dt} = \frac{\dot{\omega}}{\omega}\langle D \rangle + 2\omega\langle L \rangle - 2\kappa\langle D \rangle, \quad (\text{C4})$$

which are Eq. (8). Let us rewrite Eq. (8) into a compact form

$$\frac{d}{dt}\phi = M(t)\phi + f(t), \quad (\text{C5})$$

with the vector  $\phi = (\langle H \rangle \quad \langle L \rangle \quad \langle D \rangle)^T$  and the function  $f(t) = 2\kappa k_B T_b (1 \quad 1 \quad 0)^T$ . The matrix  $M(t)$  is

$$M(t) = \begin{pmatrix} -2\kappa + \frac{\dot{\omega}}{\omega} & -2\kappa - \frac{\dot{\omega}}{\omega} & 0 \\ -2\kappa - \frac{\dot{\omega}}{\omega} & -2\kappa + \frac{\dot{\omega}}{\omega} & -2\omega \\ 0 & 2\omega & -2\kappa + \frac{\dot{\omega}}{\omega} \end{pmatrix}, \quad (\text{C6})$$

the inverse of which is obtained as

$$M^{-1} = \begin{pmatrix} -\frac{(\frac{\dot{\omega}}{\omega}-2\kappa)^2+4\omega^2}{4(\frac{\dot{\omega}}{\omega}-2\kappa)(2\kappa\frac{\dot{\omega}}{\omega}-\omega^2)} & \frac{\frac{\dot{\omega}}{\omega}+2\kappa}{4(\omega^2-2\kappa\frac{\dot{\omega}}{\omega})} & \frac{\omega(\frac{\dot{\omega}}{\omega}+2\kappa)}{2(\frac{\dot{\omega}}{\omega}-2\kappa)(\omega^2-2\kappa\frac{\dot{\omega}}{\omega})} \\ \frac{\frac{\dot{\omega}}{\omega}+2\kappa}{4(\omega^2-2\kappa\frac{\dot{\omega}}{\omega})} & \frac{2\kappa-\frac{\dot{\omega}}{\omega}}{4(2\kappa\frac{\dot{\omega}}{\omega}-\omega^2)} & \frac{\omega}{2(\omega^2-2\kappa\frac{\dot{\omega}}{\omega})} \\ \frac{\omega(\frac{\dot{\omega}}{\omega}+2\kappa)}{2(\frac{\dot{\omega}}{\omega}-2\kappa)(2\kappa\frac{\dot{\omega}}{\omega}-\omega^2)} & \frac{\omega}{2(2\kappa\frac{\dot{\omega}}{\omega}-\omega^2)} & \frac{2\kappa\frac{\dot{\omega}}{\omega}}{(\frac{\dot{\omega}}{\omega}-2\kappa)(2\kappa\frac{\dot{\omega}}{\omega}-\omega^2)} \end{pmatrix}. \quad (\text{C7})$$

## 2. Solution of slow tuning

With the existence of the inverse  $M^{-1}$ , we rewrite the differential equation as

$$\phi = -M^{-1}f + M^{-1}\frac{d}{dt}\phi. \quad (\text{C8})$$

Using the perturbative expansion approach in Ref. [49], the solution for the slow tuning is

$$\phi = -\sum_{n=0}^{\infty} \left( M^{-1} \frac{d}{dt} \right)^n M^{-1} f, \quad (\text{C9})$$

where the time derivative  $d/dt$  acts on both  $M^{-1}$  and  $f$ . For the slow tuning satisfied

$$\frac{\dot{\omega}}{\kappa\omega} \ll 1, \quad \frac{\kappa\dot{\omega}}{\omega^3} \ll 1, \quad (\text{C10})$$

the term with  $n = 0$  dominates the summation in Eq. (C9), namely,

$$\phi \approx -M^{-1}f = k_B T_b \begin{pmatrix} \frac{\kappa[2\omega^2 + \frac{\dot{\omega}}{\omega}(\frac{\dot{\omega}}{\omega}-2\kappa)]}{(2\kappa-\frac{\dot{\omega}}{\omega})(\omega^2-2\kappa\frac{\dot{\omega}}{\omega})} \\ \frac{\kappa\dot{\omega}}{2\kappa\dot{\omega}-\omega^3} \\ -\frac{2\kappa\dot{\omega}}{(2\kappa-\frac{\dot{\omega}}{\omega})(\omega^2-2\kappa\frac{\dot{\omega}}{\omega})} \end{pmatrix}. \quad (\text{C11})$$

Keeping the first order of  $\dot{\omega}/(\kappa\omega)$ ,  $\kappa\dot{\omega}/\omega^3$ , and  $\dot{\omega}/\omega^2$ , we obtain

$$\phi^{[1]} \approx k_B T_b \begin{pmatrix} 1 + \kappa\frac{\dot{\omega}}{\omega^3} + \frac{1}{2\kappa}\frac{\dot{\omega}}{\omega} \\ -\kappa\frac{\dot{\omega}}{\omega^3} \\ -\frac{\dot{\omega}}{\omega^2} \end{pmatrix}. \quad (\text{C12})$$

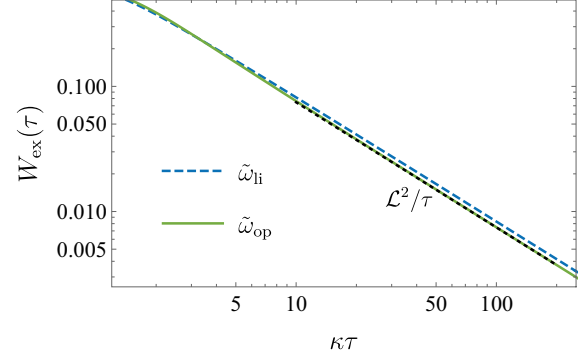


FIG. 6. The  $\tau^{-1}$  scaling of the excess work for tuning the frequency of the harmonic oscillator. We compare the excess work in the linear protocol (blue dashed curve) and the optimal protocol (green solid curve). The frequency is tuned from  $\omega_0 = 1$  to  $\omega_\tau = 2$  with the temperature  $k_B T_b = 1$ , and the dissipation rate is set as  $\kappa = 1$ . For the slow process, the lower bound of the excess work  $\mathcal{L}^2/\tau$  is given by the thermodynamic length with  $\mathcal{L} = 0.864$ .

The terms with the change of the frequency  $\dot{\omega}$  contributes to the  $\tau^{-1}$  scaling of the excess work at the long-time limit.

The power for tuning the frequency is

$$\dot{W}(t) = \frac{\dot{\omega}}{\omega}(\langle H \rangle - \langle L \rangle), \quad (\text{C13})$$

and the quasistatic work rate is  $\dot{W}_{(0)}(t) = k_B T_b \dot{\omega}/\omega$ . Plugging Eq. (C12) into the power, we obtain the excess power  $P_{\text{ex}}(t) = \dot{W}(t) - \dot{W}_{(0)}(t)$  to the lowest order of  $\dot{\omega}$  as

$$P_{\text{ex}}(t) \approx k_B T_b \frac{\dot{\omega}^2}{\omega^2} \left( \frac{1}{2\kappa} + \frac{2\kappa}{\omega^2} \right), \quad (\text{C14})$$

which leads to the thermodynamic length

$$\mathcal{L} = \int_{\omega_0}^{\omega_\tau} \sqrt{k_B T_b \left( \frac{1}{2\kappa} + \frac{2\kappa}{\omega^2} \right) \left| \frac{d\omega}{\omega} \right|}. \quad (\text{C15})$$

## 3. Numerical result of the excess work

In Fig. 6 we show the numerical result of the excess work corresponding to the inset of Fig. 2. We consider the linear protocol (blue dashed curve) with  $\tilde{\omega}_{\text{li}}(s) = \omega_0 + (\omega_\tau - \omega_0)s$  and the optimal protocol (green solid curve) with  $\tilde{\omega}_{\text{op}}(s)$  solved by Eq. (11). For the slow tuning with long duration, the excess work satisfies the  $\tau^{-1}$  scaling and is bounded by the thermodynamic length as  $W_{\text{ex}} \geq \mathcal{L}^2/\tau$ . The lower bound (black dotted line) is saturated by the optimal protocol.

## APPENDIX D: COMPRESSION OF CLASSICAL IDEAL GAS

Our recent experimental setup for validation of the  $\tau^{-1}$  scaling of the excess work with the ideal gas [54] can be used to apply the current strategy to measure the thermodynamic length. Here we show the theoretical derivation of the thermodynamic length and the excess work for the finite-time compression.

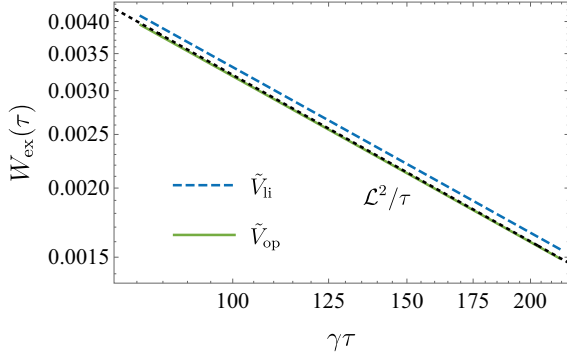


FIG. 7. The  $\tau^{-1}$  scaling of the excess work for the finite-time compression of the ideal gas. The linear protocol  $\tilde{V}_{\text{li}}(s) = V_0 + (V_\tau - V_0)s$  and the exponential protocol  $\tilde{V}_{\text{op}}(s) = V_0(V_\tau/V_0)^s$  are considered. The parameters are set as  $nR = T_b = \gamma = 1$  and  $C_V = 1.5$ , and the volume is tuned from  $V_0 = 1$  to  $V_\tau = 0.5$ . The black dotted line shows the lower bound of the excess work  $W_{\text{ex}} \geq \mathcal{L}^2/\tau$  given by the thermodynamic length  $\mathcal{L} = 0.566$ , saturated by the exponential protocol.

Defining the temperature difference  $u = T - T_b$ , we rewrite Eq. (12) as

$$\frac{du}{dt} = -\frac{nR}{C_V}(T_b + u)\frac{\dot{V}}{V} - \gamma u. \quad (\text{D1})$$

The series expansion solution is obtained as

$$u = \sum_{n=0}^{\infty} \left( -\frac{1}{\frac{nR}{C_V}\frac{\dot{V}}{V} + \gamma} \frac{d}{dt} \right)^n \left( \frac{-\frac{nRT_b}{C_V}\frac{\dot{V}}{V}}{\frac{nR}{C_V}\frac{\dot{V}}{V} + \gamma} \right). \quad (\text{D2})$$

The power of the compression is  $\dot{W} = -p\dot{V} = -nRT\dot{V}/V$ . In the quasistatic process, the temperature of the gas is the same as that of the bath, i.e.,  $T = T_b$ , and the quasistatic work rate is  $\dot{W}_{(0)}(t) = -nRT_b\dot{V}/V$ . For the slow tuning  $nR\dot{V}/(\gamma C_V V) \ll 1$ , the term with  $n = 0$  dominates the summation in Eq. (D2), and the temperature difference to the lowest order is  $u^{[0]} = -nRT_b\dot{V}/(\gamma C_V V)$ . The excess power  $P_{\text{ex}} = \dot{W} - \dot{W}_{(0)}(t)$  approximates

$$P_{\text{ex}} \approx \frac{(nR)^2 T_b}{\gamma C_V} \left( \frac{\dot{V}}{V} \right)^2, \quad (\text{D3})$$

with the excess work

$$W_{\text{ex}} \approx \int_0^\tau \frac{(nR)^2 T_b}{\gamma C_V} \left( \frac{\dot{V}}{V} \right)^2 dt. \quad (\text{D4})$$

The thermodynamic length follows as

$$\mathcal{L} = \int_0^\tau \sqrt{\frac{(nR)^2 T_b}{\gamma C_V} \left( \frac{\dot{V}}{V} \right)^2} dt, \quad (\text{D5})$$

which gives Eq. (14).

In Fig. 7 we show the numerical result of the excess work for the finite-time compression of ideal gas. The excess work exhibits the  $\tau^{-1}$  scaling during the slow compression process. The compression with the exponential protocol (green solid curve) consumes the lower excess work compared to that of the linear protocol (blue dashed curve) with the given duration

$\tau$ . The lower bound  $\mathcal{L}^2/\tau$  (black dotted line) is saturated by the optimal protocol as the exponential protocol.

### 1. Errors in measurements

In experiments, the pressure  $p(t)$  of the gas and the volume of the cavity  $V(t)$  are measured during the compression [54]. According to Eq. (3), the finite-time thermodynamic length is obtained through

$$\mathcal{L}(\tau) = \int_0^\tau \sqrt{-\left[ p(t) - \frac{p(0)V(0)}{V(t)} \right] \dot{V}(t)} dt. \quad (\text{D6})$$

Yet errors inevitably exist in the measurements, and hinder to extract the precise result of the thermodynamic length. The effect of the errors is more remarkable with a longer duration, since the excess power becomes too small to be measured. As an illustration, we consider the measurements of the pressure contain two kinds of errors, the systematic error (caused by the pressure sensor calibration) or the random error (caused by the electronic noise of devices).

(1) *Systematic error*: If the systematic error exists, the measured pressure is

$$p_{\text{mea}}(t) = p_{\text{real}}(t) + \delta p. \quad (\text{D7})$$

With  $10^{-5}$  systematic error in the pressure, the long time limits of the measured finite-time thermodynamic length deviates from the thermodynamic length (horizontal black dashed line), as shown by the thin curves in Fig. 3. We take the real part of the finite-time thermodynamic length since the square root may be imaginary induced by the error.

(2) *Random error*: We consider the measured pressure contains the random error

$$p_{\text{mea}}(t) = p_{\text{real}}(t) + \Delta p(t). \quad (\text{D8})$$

To reveal the effect of  $\Delta p(t)$ , we simulate it as a Gaussian white noise with the standard deviation  $\sigma = 10^{-3}$  and zero mean value  $\langle \Delta p(t) \rangle = 0$ . We assume the pressure is measured with the interval  $\delta t = 0.1$ . The measured pressure is considered as the interpolation by Eq. (D8) with  $\Delta p(t)$  at

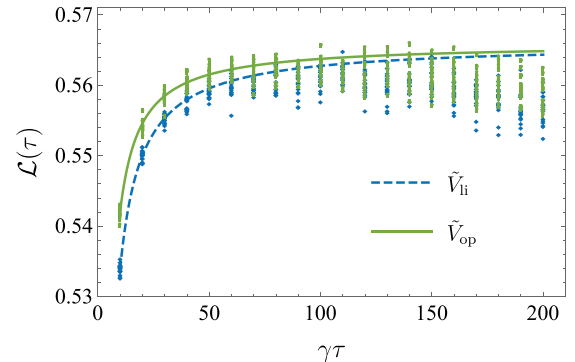


FIG. 8. The measured finite-time thermodynamic length  $\mathcal{L}(t)$  with the random error. The standard deviation of the random error is  $\sigma = 10^{-3}$ . The solid and the dashed curves present the extrapolation functions of the optimal and the linear protocols, while the markers show the corresponding simulated results with the random errors.

each moment. Notice that the random error  $\Delta p(t)$  may also lead to the imaginary square root. The real part of the finite-time thermodynamic length is shown in Fig. 8. The solid and the dashed curves present the extrapolation functions of the optimal and the linear protocols, while the markers show the corresponding simulated results with the random errors. For

each operation time  $\tau$ , we simulate the compression process 20 times, where in each time we generate a different random error  $\Delta p(t)$ . The results show that the effect of the random error increases with the longer operation time  $\tau$ , which hinders the precise measurement of the finite-time thermodynamic length of slow isothermal processes.

- [1] B. Andresen, P. Salamon, and R. S. Berry, *Phys. Today* **37**, 62 (1984).
- [2] R. S. Berry, V. A. Kazakov, S. Sieniutycz, Z. Szwast, and A. M. Tsvilin, *Thermodynamic Optimization of Finite-Time Processes* (John Wiley & Sons, Chichester, 2000).
- [3] B. Andresen, *Angew. Chem. Int. Ed.* **50**, 2690 (2011).
- [4] V. Cavina, A. Mari, A. Carlini, and V. Giovannetti, *Phys. Rev. A* **98**, 052125 (2018).
- [5] K. Proesmans, J. Ehrlich, and J. Bechhoefer, *Phys. Rev. Lett.* **125**, 100602 (2020).
- [6] F. L. Curzon and B. Ahlborn, *Am. J. Phys.* **43**, 22 (1975).
- [7] P. Salamon, A. Nitzan, B. Andresen, and R. S. Berry, *Phys. Rev. A* **21**, 2115 (1980).
- [8] J. Chen, *J. Phys. D: Appl. Phys.* **27**, 1144 (1994).
- [9] C. Van den Broeck, *Phys. Rev. Lett.* **95**, 190602 (2005).
- [10] Z. C. Tu, *J. Phys. A: Math. Theor.* **41**, 312003 (2008).
- [11] M. Esposito, R. Kawai, K. Lindenberg, and C. Van den Broeck, *Phys. Rev. Lett.* **105**, 150603 (2010).
- [12] A. Ryabov and V. Holubec, *Phys. Rev. E* **93**, 050101(R) (2016).
- [13] N. Shiraishi, K. Saito, and H. Tasaki, *Phys. Rev. Lett.* **117**, 190601 (2016).
- [14] V. Cavina, A. Mari, A. Carlini, and V. Giovannetti, *Phys. Rev. A* **98**, 012139 (2018).
- [15] Y.-H. Ma, D. Xu, H. Dong, and C.-P. Sun, *Phys. Rev. E* **98**, 042112 (2018).
- [16] P. Abiuso and M. Perarnau-Llobet, *Phys. Rev. Lett.* **124**, 110606 (2020).
- [17] F. Weinhold, *J. Chem. Phys.* **63**, 2479 (1975).
- [18] P. Salamon, J. D. Nulton, and R. S. Berry, *J. Chem. Phys.* **82**, 2433 (1985).
- [19] G. Ruppeiner, *Rev. Mod. Phys.* **67**, 605 (1995).
- [20] G. E. Crooks, *Phys. Rev. Lett.* **99**, 100602 (2007).
- [21] M. Scandi and M. Perarnau-Llobet, *Quantum* **3**, 197 (2019).
- [22] P. Abiuso, H. J. D. Miller, M. Perarnau-Llobet, and M. Scandi, *Entropy* **22**, 1076 (2020).
- [23] L. Diósi, K. Kulacsy, B. Lukács, and A. Rácz, *J. Chem. Phys.* **105**, 11220 (1996).
- [24] P. R. Zulkowski and M. R. DeWeese, *Phys. Rev. E* **92**, 032113 (2015).
- [25] Y.-H. Ma, D. Xu, H. Dong, and C.-P. Sun, *Phys. Rev. E* **98**, 022133 (2018).
- [26] M. V. S. Bonança and S. Deffner, *J. Chem. Phys.* **140**, 244119 (2014).
- [27] Y. Zhang, *Europhys. Lett.* **128**, 30002 (2020).
- [28] P. Salamon and R. S. Berry, *Phys. Rev. Lett.* **51**, 1127 (1983).
- [29] J. Nulton, P. Salamon, B. Andresen, and Q. Anmin, *J. Chem. Phys.* **83**, 334 (1985).
- [30] D. A. Sivak and G. E. Crooks, *Phys. Rev. Lett.* **108**, 190602 (2012).
- [31] T. Van Vu and Y. Hasegawa, *Phys. Rev. Lett.* **126**, 010601 (2021).
- [32] M. Esposito, U. Harbola, and S. Mukamel, *Rev. Mod. Phys.* **81**, 1665 (2009).
- [33] K. Maruyama, F. Nori, and V. Vedral, *Rev. Mod. Phys.* **81**, 1 (2009).
- [34] R. Kosloff, *Entropy* **15**, 2100 (2013).
- [35] S. Vinjanampathy and J. Anders, *Contemp. Phys.* **57**, 545 (2016).
- [36] D. P. Pires, M. Cianciaruso, L. C. Céleri, G. Adesso, and D. O. Soares-Pinto, *Phys. Rev. X* **6**, 021031 (2016).
- [37] P. Strasberg, G. Schaller, T. Brandes, and M. Esposito, *Phys. Rev. X* **7**, 021003 (2017).
- [38] L. Mancino, V. Cavina, A. De Pasquale, M. Sbroscia, R. I. Booth, E. Rocca, I. Gianani, V. Giovannetti, and M. Barbieri, *Phys. Rev. Lett.* **121**, 160602 (2018).
- [39] H. J. D. Miller and M. Mehboudi, *Phys. Rev. Lett.* **125**, 260602 (2020).
- [40] P. R. Zulkowski, D. A. Sivak, G. E. Crooks, and M. R. DeWeese, *Phys. Rev. E* **86**, 041148 (2012).
- [41] G. M. Rotskoff and G. E. Crooks, *Phys. Rev. E* **92**, 060102(R) (2015).
- [42] D. A. Sivak and G. E. Crooks, *Phys. Rev. E* **94**, 052106 (2016).
- [43] E. H. Feng and G. E. Crooks, *Phys. Rev. E* **79**, 012104 (2009).
- [44] H.-P. Breuer and F. Petruccione, *The Theory of Open Quantum Systems* (Oxford University Press, Oxford, 2007).
- [45] R. Alicki, *J. Phys. A: Math. Gen.* **12**, L103 (1979).
- [46] H. T. Quan, Y. X. Liu, C. P. Sun, and F. Nori, *Phys. Rev. E* **76**, 031105 (2007).
- [47] D. Mandal and C. Jarzynski, *J. Stat. Mech.* (2016) 063204.
- [48] G. E. Crook, <https://threeplusone.com/pubs/drazin03/>.
- [49] V. Cavina, A. Mari, and V. Giovannetti, *Phys. Rev. Lett.* **119**, 050601 (2017).
- [50] C. Jarzynski, *Phys. Rev. Lett.* **78**, 2690 (1997).
- [51] A. Caldeira and A. Leggett, *Physica A* **121**, 587 (1983).
- [52] Y. Rezek and R. Kosloff, *New J. Phys.* **8**, 83 (2006).
- [53] S. Lee, M. Ha, J.-M. Park, and H. Jeong, *Phys. Rev. E* **101**, 022127 (2020).
- [54] Y.-H. Ma, R.-X. Zhai, J. Chen, C. P. Sun, and H. Dong, *Phys. Rev. Lett.* **125**, 210601 (2020).
- [55] Z. Gong, Y. Lan, and H. T. Quan, *Phys. Rev. Lett.* **117**, 180603 (2016).
- [56] S. An, M. Um, D. Lv, Y. Lu, J. Zhang, H. Quan, Z. Yin, J. N. Zhang, and K. Kim, *Nat. Phys.* **11**, 193 (2014).
- [57] J. Rosznagel, S. T. Dawkins, K. N. Tolazzi, O. Abah, E. Lutz, F. Schmidt-Kaler, and K. Singer, *Science* **352**, 325 (2016).